Nuclear Engineering and Design 295 (2015) 138–147

Contents lists available at ScienceDirect

Nuclear Engineering and Design

journal homepage: www.elsevier.com/locate/nucengdes

Influence of the wet-well nodalization of a BWR3 Mark I on the containment thermal-hydraulic response during an SBO accident

Luis E. Herranz*, Joan Fontanet, Elena Fernández, Claudia López

Unit of Nuclear Safety Research, CIEMAT, Av. Complutense 40, 28040 Madrid, Spain

HIGHLIGHTS

- Analysis of SBO sequences in BWR3 Mark I containments.
- Multiple-mesh nodalization allows pool stratification set up.
- Mass, momentum and energy exchanges between nodes play a key role.
- Validation/verification against a scaled-down database required to credit meshing schemes.

ARTICLE INFO

Article history:
Received 28 January 2015
Received in revised form 10 June 2015
Accepted 10 September 2015

ABSTRACT

In the field of severe accidents simulation one of the most challenging issues is nodalization. This paper explores the effect of the wet well modeling on significant variables describing the sequence evolution. The code used for the study has been MELCOR 2.1 and the scenario chosen has been a prolonged SBO occurring in a BWR3 Mark I. The results indicate that some significant magnitudes show a moderate scatter depending on WW nodalization (i.e., core uncovery, RPV failure, hydrogen production), whereas the SP thermal state might display outstanding deviations, which sometimes affect significantly key variables like containment pressure. The difficulties and uncertainties around defining a suitable WW nodalization have been highlighted and the need to properly balance the entire plant meshing has been stressed.

Even though a number of noding schemes has been explored, the results discussion underlines the importance of having a deep understanding of the potential phenomena governing the scenario and of mastering the code facilities to better model it. Some insights into WW nodalization in MELCOR 2.1 have been gained for the specific scenario (i.e., a prolonged SBO in a BWR3 Mark I) explored: a single node assumption might underestimate PCV pressurization; a loose coupling of water and gas exchanges in the WW nodalization would be preferred if the drift flux model is chosen for momentum exchange in the flow pathways between WW nodes; the potential of some axial thermal stratification in the pool should be taken into account when noding the WW; sensitivity analyses on physically supported WW nodalization schemes should be conducted and focused on key magnitudes describing containment evolution (i.e., pressure). Finally, it is stated that some uncertainties in WW nodalization might be reduced and/or moved if a properly scaled-down experimental project was launched on potential stratification in BWR3 Mark I SP during SBO accidents.

1. Introduction

The Fukushima accident revived the interest worldwide for severe accidents and fostered assessments of NPPs (nuclear power plant) capability to withstand threats resulting from accidents beyond those used as a basis for NPP design (BDBA, beyond design-basis accidents). In Japan, where all the NPPs where shut down right after the March 11, 2011, NPP safety has been under evaluation according to new and even more stringent regulations; at present 17 out of 48 nuclear reactors have submitted their applications for restart. In the European Union, the 132 NPP underwent stress tests and peer reviews in 2011 and 2012 (many other countries, like Switzerland, Ukraine, Russia and others, followed the European path and adopted similar methodologies). The generic conclusion was that there were not technical reasons requiring the shutdown of any NPP in Europe (EC, 2012). Nonetheless, practically

* Corresponding author. Tel.: +34 913 466 219; fax: +34 913 466 233.
E-mail address: luisen.herranz@ciemat.es (L.E. Herranz).

http://dx.doi.org/10.1016/j.nucengdes.2015.09.031
0029-5493/

all NPPs have been required to implement technical upgrades that should enhance safety even further. Examples of them are installation of FCVs (filtered containment venting) and/or PARs (passive autocatalytic recombiner), in many of those NPPs that did not have it yet.

Severe accident research has been also heavily affected by the Fukushima accident. In addition to domestic Japanese projects dealing with numerous issues raised by the accidents, like pool scrubbing (Mizokami et al., 2014), a number of international projects have been launched, the flagship of which is likely OECD/NEA BSAF; its main purpose is to achieve a thorough understanding of the severe accidents evolutions in Units 1 through 3 and to contribute to improvement of methods and models of the severe accident codes and to their validation (NEA, 2012). Under the 7th European Framework Program, projects like PASSAM (Herranz et al., 2014) and CESAM (Van Dorsselaere et al., 2015) are intimately linked to specific aspects that were relevant during the Fukushima accident. The former is investigating potential enhancement of filtration efficiency under containment venting conditions; the latter is extending the ASTEC code application domain and this includes the SFP (spent fuel pool) accident scenarios.

The CESAM project is just an example of the many activities ongoing aimed at enhancing predictability of severe accident codes. Benchmarking codes against data from experiments addressing scenarios that had relevance or raised concerns during the Fukushima accident (NEA, 2013) and developing new models for phenomena potentially involved in reactor and SFP accident scenarios (Birchley and Fernández-Moguel, 2012), are two of the main tracks in which analytical efforts are being conducted. All of these activities have a common goal: to reduce uncertainties in code predictions as much as feasible and, no less important, being aware of the range of such uncertainties. However, no matter how complete and sophisticate codes and models become, there will always be an intrinsic uncertainty associated to users, the so called “user effect”, which so many times have been discussed (Jones et al., 2003; Clément and Haste, 2004). This user effect is articulated through the codes input decks and there are three major areas on which it may take place: the physical models (i.e., choice among several models; selection of model parameters; activation/deactivation of models, etc.); the working systems (i.e., settings for safety systems performance); and the plant and/or facility nodalization (i.e., spatial discretization of the plant). The latter is the main focus of this article.

The nodalization has been demonstrated to affect modeling of key phenomena in the containment of a NPP undergoing a severe accident. An example is hydrogen distribution and the potential development of dissolution of atmosphere stratifications, which requires nodalizations with sufficient detail in the vertical direction and definition of nodes and flow paths (FP) capable of capturing gas plumes moving upward (Schwarz et al., 2011). Another one is the gaseous iodine–steel interactions, which has been shown to be a function of the isotope local concentration and, as a consequence, affected by the way the vessel is meshed and the in-between nodes junctions defined (Weber et al., 2013). And, finally, a no less significant example is the wet well pool stratification, which has been recently the focus of experimental (Laine et al., 2011) and theoretical studies (Zhao et al., 2014), given its relevance during accidents in BWR (boiling water reactor) as a major thermal energy sink within the containment and a key source of cooling water for the reactor core. This significance was the trigger to investigate the effect of wet well (WW) nodalization in severe accident progression in the present paper.

An accurate prediction of the thermal state of BWR suppression pools (SP) is important because, in the course of an accident, it affects the peak containment pressure and, if existing (depending on BWR designs) and available, the performance of safety systems, like the RCIC (Reactor Core Isolation System) and HPCI (high pressure coolant injection). A number of previous analyses assumed a simple containment nodalization when analyzing accidents in BWR Mark I NPPs (Lee and Lee, 1992; Carbajo, 1994) and even some recent works (Park and Ahn, 2012) seem to follow that path. However, this is a strong hypothesis that was already questioned in the 70s and 80s of last century. At the time, the major concern was the vibratory loads on containment structures that potential instability of steam condensation might cause when extensive steam was blowdown during transients from the RPV (reactor pressure vessel) through SRVs (safety-relief valve) (Su, 1981). An extensive experimental and analytical research was conducted. Experimental data were taken in nuclear power plants, like Monticello NPP, to find out effective designs of quenchers and discharge systems of RHR (Residual Heat Removal) to enhance thermal mixing in the suppression pool during transients (Patterson, 1979). These experiments were the bases to validate sophisticated pool models other than the traditionally assumed single, well-mixed model, which was stated not to be suitable under severe SBO (Station Blackout) accidents (Cook, 1984). Those models required the suppression pool splitting into a good number of nodes (even more than 70) and consisted in sub-models that applied to different regions of the water pond: convection cells vs. thermal stratification for the discharge bay, depending on the initial momentum of injected steam; bulk circumferential circulation in the entire pool for the fluid far field motion; and a uniform whole pool mixing, when steam injection occurred energetically at different locations of the pool.

This work has been focused on studying the effect of the wet well modeling with a modern lumped parameter code (i.e., discretization and flow path definition) on primary containment variables, like pressure. The code used for the study has been MELCOR 2.1 and the scenario chosen has been a prolonged SBO occurring in a BWR3 Mark I, which has turned out to be one of the most challenging scenarios to model for a lumped parameter code.

2. Description of the scenario

There are a number of mid-size boiling water reactors of a GE design similar to Unit 1 at the Fukushima Daiichi site (BWR3 Mark I, 1380 MW_{th}) around the world. This type of plant has been chosen for the present study. The accident scenario to be investigated is an SBO (i.e., a total loss of on-site and off-site alternate current power). The interest of SBOs is beyond any doubt: SBOs dominate contribution to CDF (core damage frequency) in BWRs (U.S. NRC, 2005); but, more importantly, it was the loss of electric power to normal and emergency core cooling systems and the subsequent failure of back-up decay heat removal systems what compromised water injection in the cores of the Units 1–3 at the Fukushima-Daiichi NPP (NAIIC, 2012).

In the WASH-1400 report (U.S. NRC, 1975), SBOs were highlighted as important contributors to the total risk from NPP accidents. As a consequence, they were largely explored in the late 80s to 90s (Carbajo, 1994; Hanson et al., 1988; Lee and Lee, 1992; Ott, 1989) and most of that research got encapsulated in NUREG-1150 (U.S. NRC, 1990). More recently, further work with more capable analytical tools, like the last versions of the MELCOR code, has updated the insights earlier gained (Leonard et al., 2007; Gauntt et al., 2012; Herranz et al., 2012a, 2012b). The SOARCA report might be seen as a good compilation of such progress (Bixler et al., 2013).

In the case of a STSBO (Short Term Station Blackout) accident, both AC and DC power are lost, so that all turbine-driven systems become unavailable in the short run. With reactor control blades, MSIVs (main steam isolation valve), and containment isolation valves at their fail-safe positions (inserted and closed), the only systems available for decay heat removal from the core are ICs

Table 1
Key events and timing in the RPV (8-node 1 flow path).

Key event	Time (h)
IC working period	0–1.2
SRV working period	1.6–14.9
Core uncovery	3.2–5.3
Fuel slump to lower plenum	6.3
Dry RPV	10.7
Vessel breach	14.9

(isolation condenser) and SRVs. The first ones are safety-related systems that allow core cooling when reactor is isolated from turbine and condenser. They condense the steam being produced in the RPV and return the resulting condensate to the vessel. The second ones are installed on the main steam lines and protect the RCS (Reactor Coolant System) against over-pressure transients and allow water injection at low pressure when operated as the ADS (automatic depressurization system). The SRS (safety relief system) consists of SRVs discharging into the SP and SVs (Safety Valve) discharging into the DW (dry well). Its design (i.e., number of valves and setpoints) is plant specific and usually entails staggered setpoints of individual valves that make them open sequentially. In this study a generic system has been modeled, with 4 SRVs and 3 SVs, which setpoints have been defined accordingly with pressure levels prototypical of BWR3 Mark I NPPs. Valves are modeled to open when the pressure reaches the setpoint values. Both systems, IC and SRVs, are assumed to come into play at pressures above 7.3 MPa in the RPV, the IC being the first one brought into operation (SVs have the highest pressure setpoints).

The ICs (2 units) have been operating during the first 1.2 h of the sequence (according to the modeling described in next section). No water has been injected in the reactor, assuming no power is available at the time. Once the ICs stop, the water in the vessel heats up till reaching saturation conditions; water evaporation increases RCS pressure. As a result, the SRV with the lowest setpoint opens to keep pressure under control; the steam released is driven to the WW, where most of it condenses. Other SRVs do not open since pressure is kept always below their setpoints. Core uncovery starts a little later than 3 h after the scram and it lasts more than 2 h. As a consequence, the core degrades and a substantial amount of hydrogen is released (more than 600 kg until RPV failure) together with fission products and aerosols. Core temperatures peak at nearly 2800 K.

Oxidation of cladding, metal and control rod materials began at around 4 h, although it speeded up later on, when a good fraction of the core got exposed to steam. The highest oxidation period lasts until more than 6 h when most of the fuel slumped into the lower plenum (around 70%). Despite most H_2 generated came from Zircaloy oxidation (69%), other materials oxidation contributed significantly too (more than 200 kg).

In order to give an overall view of the accident progression, Table 1 shows the timing of key events corresponding to a specific case, the one characterized by 8 WW nodes with just a single flow path connecting adjacent nodes (8 node 1 flow path), as it will be described below.

3. Plant modeling

The sequence has been simulated with the MELCOR 2.1 code (Gauntt et al., 2011). MELCOR is a fully integrated, engineering-level computer code that models the progression of severe accidents in light water reactors. It includes a broad spectrum of phenomena, from core degradation to source term to the environment; just to mention a few: thermal-hydraulic response in the reactor coolant system, reactor cavity, containment, and confinement buildings; core heatup, degradation, and relocation; core-concrete attack; hydrogen production, transport and combustion; fission product release, transport and behavior. Given the nature of the present investigation, this article focuses on two major aspects of sequence modeling: nodalization and associated thermal-hydraulic phenomena.

Particularly relevant for this study are the MELCOR 2.1 approximations to steam injection in the discharge control volume and to the fluid flow through flow paths. There is not a sparger model in MELCOR so that mass and energy discharged are assumed to be uniformly distributed in the receiving control volume. This entails two major deviations from reality: a lower water temperature in the receiving node due to overestimation of water heat capacity because all the mass in the node is considered, and an instantaneous temperature increase in the water volume. Concerning mass and energy advected through flow paths (no mass or energy is associated with a flow path), whenever water and gas are transported through, MELCOR uses a version of the so called “drift flux” model (Wallis, 1969). It considers a single momentum equation defining an average mixture velocity for the two fields and modeling the relative velocity between them as a constitutive relation.

In next sections a thorough description of plant meshing, particularly WW modeling, is given. Note that no RPV-to-PCV potential leakages have been assumed. The time span explored in the present study extends from the reactor scram until the RPV failure.

3.1. Plant nodalization

The entire NPP has been modeled. Large components and buildings, like RPV, DW, WW and RB (reactor building), have been split into nodes; *ad-hoc* models for safety related systems (i.e., IC and SRVs) have been built according to their performance specifications. A total number of 73 nodes have been used for the plant description. Even though RB has been described through 10 volumes, in the present study connections between DW/WW and RB (i.e., leaks) and between DW/WW and environment (i.e., venting), have been kept closed. The specific pressure levels of venting and PCV (primary containment vessel) failure will be noted in the presentation of results to emphasize the potential consequences of different nodalizations.

The RPV has been split into 38 thermal-hydraulic control volumes. Individual control volumes have been used for steam dome, dryers, separators, shroud dome, annulus and lower plenum. Unlike them, the core active region has been meshed in 32 volumes: 4 radial regions, in each of which there are a bypass region (simulating in-between canister spacing and in-assembly water rods) and a channel region; the latter has been split, in turn, in 7 axial nodes. This meshing is more detailed than the classical approach of using one single node for all the channels (Carbajo, 1994; Herranz et al., 2012b), so that a closer approximation to the in-core fluid thermal map might be achieved. As for the specific nodalization to track core degradation, a similar scheme has been used except in the lower plenum: an additional radial zone (the region right under the annulus) has been added and 4 axial regions have been considered from the RPV bottom to the lower core support plate. This meshing should be sufficient for a detailed description of major phenomena affecting fuel (oxidation, melting, relocation, etc.). Fig. 1 displays the nodalizations for both the thermal-hydraulic and the core degradation analyses.

The DW (~3000 m^3) is 9-node network (Fig. 2a). Axially 3 regions have been considered: lower, mid and upper zones. The lower region is the one located from the DW floor to the RPV bottom height. It consists of 3 nodes: the inner cavity region, right below the RPV, is connected to the “outer” lower DW space through a single slit; and two azimuthally symmetric regions that divide the outer lower DW region to account for the potential impact of the slit facing the cavity (note that this feature is unimportant in this study

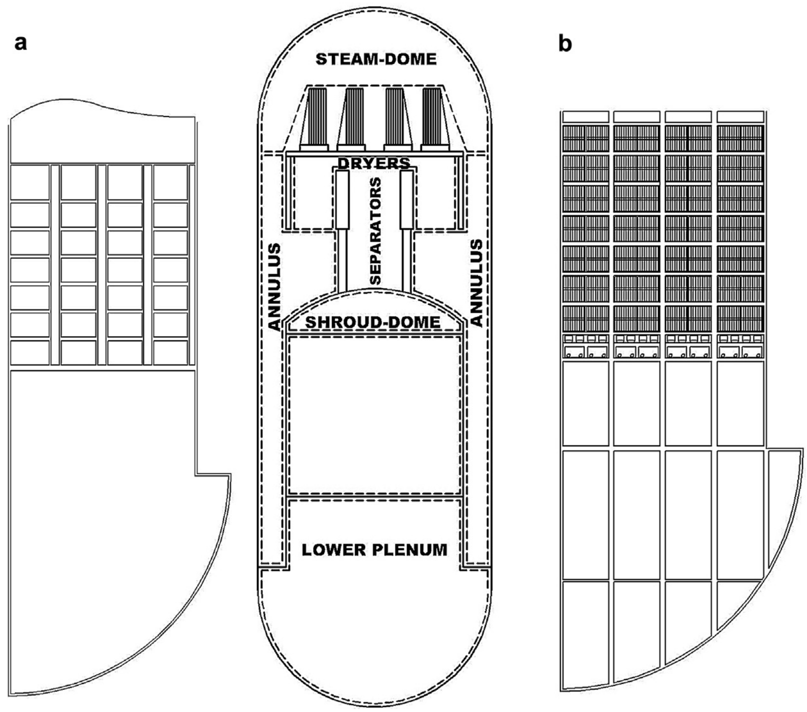

Fig. 1. RPV nodalization schemes. (a) Thermal-hydraulic meshing. (b) Core meshing.

since the analysis extends until RPV breach). The mid-section of the DW has been divided in 4 nodes: 2 symmetrical azimuthal nodes (as in the lower region) that, in turn, break down into 2 radial nodes, one of which faces the RPV external surface and the other does the PCV inner surface. The upper region is the one surrounding the RPV head and, as the others, it has been split in two azimuthal nodes. This arrangement and the appropriate junctions between volumes, allow natural convection cooling of the external RPV walls.

Vents and VBs (Vacuum Breakers) between DW and WW have also been considered. Vents have been modeled as 8 nodes with flow paths linking with both DW and WW; the flow paths have been directed *ad-hoc* DW–vent and vent–WW (in-pool injection with an initial submergence of ~1.5 m). Vacuum breakers have been defined as 8 WW to DW valve-controlled flow paths (valves open when pressure difference is over 3.5 kPa roughly). It is worth noting that VB performance is linked to the WW modeling. The local pressure difference between WW and DW is dependent on the nodalization scheme, as the latter (along with the way of connecting neighbor WW nodes through flow paths) affects the distribution of gases between adjacent nodes and, consequently, the pressure accumulation in each individual node. Namely, if the node-to-node connection in a specific WW nodalization scheme results in a fast gas mass transfer, WW pressure will become uniform almost instantaneously and in case of WW–DW pressure differences over the VB threshold, all the VBs in the individual nodes will open at the same time. Contrarily, if gas transfer between adjacent nodes is slow compared to mass flow rate coming into the receiving node atmosphere, it will be the VB in this receiving node the one which will be mostly responsible for the WW–DW pressure equalization.

Given the specific goal of this paper, WW modeling is individually described next.

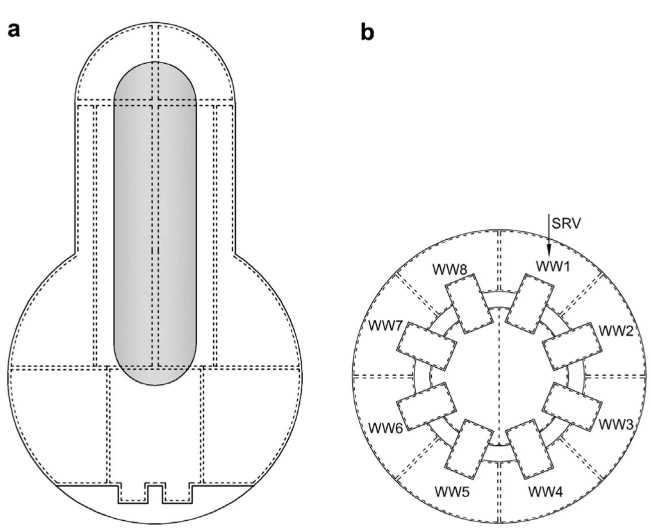

Fig. 2. PCV nodalization schemes. (a) DW. (b) 8-node WW.

3.2. Wet well modeling

Two specific features of wet well modeling are of significance in this study: WW meshing and flow paths definition in between nodes.

Three fundamental WW nodalization schemes have been tested (some more will be added as parametric studies):

- Single node. The entire WW volume (~4500 m^3) has been considered one node, with the suppression pool (~40% of the total volume) as the liquid phase and the gas over the pool surface as the gas phase. Each of these phases is assumed to be well-mixed.
- Eight circumferential nodes. The WW has been split according to DW/WW vents arrangement; that is, the whole WW volume has been divided in 8 identical nodes, among which the only differences are their azimuthal location and the fact that SRV discharge in some of them. Fig. 2b displays this WW configuration.
- Sixteen (8×2) nodes. Based on the 8-node arrangement, volumes have been vertically broken in an upper node, whose composition is gas, and a lower node, mostly consisting of water and a thin layer of gas over the interface.

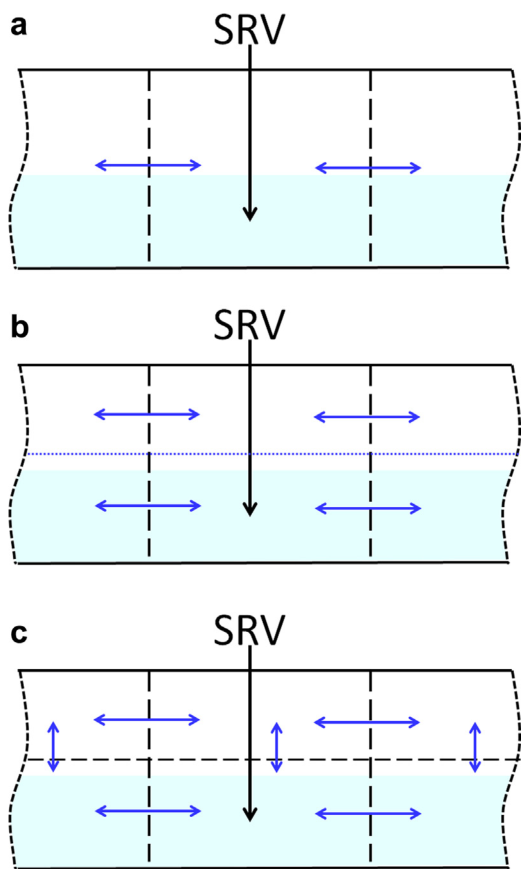

Fig. 3. Flow path schematics. (a) Single flow path. (b) Double flow path. (c) 8 × 2-node flow path.

By comparing the first two configurations the potential for circumferential stratification has been explored. An instantaneous uniform distribution of heat and mass loads in the SP (1-node configuration), might result in a pool thermal state drastically different from a local discharge (8-node configuration). In the latter arrangement, a uniform thermal state might not happen and/or might take long. Nonetheless, splitting "open volumes" requires defining how individual meshes relate with each other; as a consequence, modeling uncertainties come up regarding the way such interconnection is defined. In other words, flow paths become an essential ingredient of the modeling.

Two types of node-to-node connection have been defined in the 8-node configuration: a "single flow path" (Fig. 3a), which covers the entire torus cross section and allows both phases move at different velocities and exchange momentum (Gauntt et al., 2011); a "double flow path" (Fig. 3b), in which the upper one transfers just gas between adjacent compartments and the lower one carries mainly water and a thin (≤30 cm) gas layer. The latter has been tried to avoid a potential overestimate of gas–water momentum exchange between both phase bulks due to their different density. Main geometric characteristics of the flow path in each configuration are given in Table 2. The third configuration given above (8 × 2 nodes) would stress this phase separation even further.

Table 2
Main characteristics of flow paths.

Approach	Length (m)	Cross section (m^2)
Single flow path	11.5	50
Double flow path	11.5	20 (lower) 30 (upper)

In all the cases, flow paths have been defined through the default values recommended by Gauntt et al. (2011): coefficients for form loss pressure (1.0) and laminar flow (16.0); and surface roughness of 5×10^{-5} m. The flow path lengths have been approximated as the center-to-center distance. It is worth noting that this same value has been assumed for the pool/atmosphere momentum exchange length (default option), although it is known that such a choice tends to overpredict the coupling between gas and liquid phases (Gauntt et al., 2011).

Each WW node includes two heat structures (HS) with a "pipe-like HS element": one simulates the lower part of WW torus and it is completely submerged; the other accounts for the dry section of the torus plus the internal structures and it is partially submerged (around 20% of the total surface area). Note that the latter entails a "heat bridge" between gas and water phases in the node. This configuration is generic and it has been used in all the nodalization schemes except for the 8 × 2 nodes one. In this specific arrangement heat structures are split into wet and dry ones, so that there is not a "structure heat bridge" between phases. In other words, whenever a partially immersed HS exists in a WW node heat transfer between gas and water is enhanced with respect to the alternative used in the 8 × 2 nodalization scheme, where such gas–water heat transfer cannot occur through any shared HS.

3.3. Safety systems

The two safety systems of relevance in the sequence are the SRVs and the ICs.

The SRVs performance through a pressure hysteresis cycle has been modeled by valve flow paths between the RPV and the SP (with ~2.0 m submergence). Four SRVs have been modeled and their set-points given through control functions, so that they would open sequentially if, once the lowest setpoint is reached, pressure keeps on rising and attaining the other ones. However, in the present study only the lowest setpoint is reached and just one SRV is predicted to open. Each SRV pipe connecting RPV and WW, discharges steam and non-condensibles in a different azimuthal location of the suppression pool (8 and 8 × 2 node configurations); mass and energy exchange between gas and pool is calculated based on the pool scrubbing module in MELCOR 2.1 (i.e., SPARC90).

A single IC unit has been modeled with the total capacity of the 2 existing units (about 85 MW) in the generic NPP. As IC performance preserves the total water inventory in the RPV, the IC model has been based on an enthalpy withdrawal from the vessel: once the IC starts, steam latent heat is removed from the RPV according to an IC efficiency that is a function of the RPV pressure (Gauntt et al., 2012). The IC comes into operation when RPV pressure reaches 7.3 MPa and it stops under any of the following conditions: in-dome steam mass fraction lower than 0.5, steam temperature higher than 20 K over saturation (i.e., superheated steam) or water level in the secondary side of heat exchanger below 0.8 m from the bottom of the component. No water is supplied to the IC cask during the sequence, so that after some time working, the IC stops and is no longer available.

4. Major insights

As described in Section 3.2, this study has been based on a number of analyses whose comparison sheds light on the WW modeling effect on an SBO analysis in BWR3 Mark I reactors. Particularly, the potential impact of nodalization and definition of node-to-node connections have been explored. Fig. 4 displays a conceptual flowchart of the studies conducted. As noticed, a total of five scenarios (those highlighted in blue) have been explored.

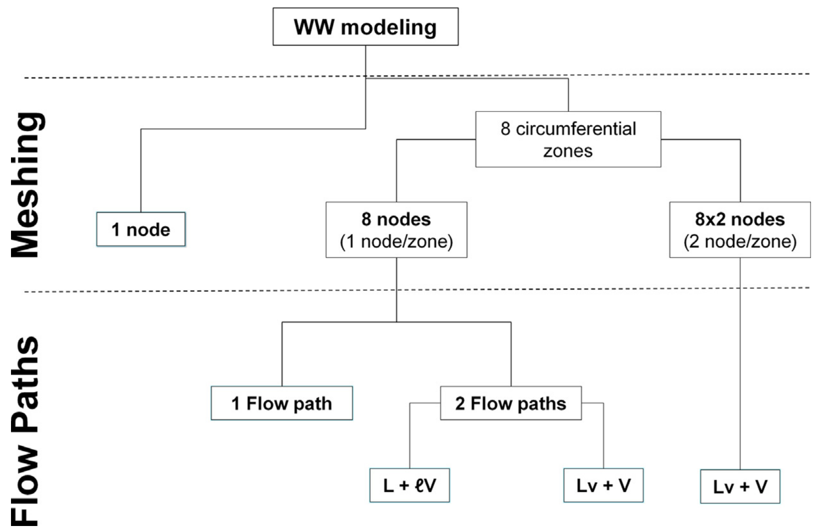

Fig. 4. Flowchart of the study rationale.

The two flow path configuration allows two arrangements: Lv+V,[1] one flow path through which fluid consists mostly of water but with a layer of gas over the liquid phase and the upper flow path that transports 100% gas; and L+ℓV,[1] which is just the reverse (the lower flow path as a pure liquid pipe and the upper one through which most cross section is full of gas with a minor, but mass-significant, film of water). The 8 × 2 node case has been run with the Lv+V flow path arrangement.

It is worth emphasizing that the present work has been focused on circumferential WW splitting since it is illustrative enough of the significance of WW nodalization when modeling an SBO accident. This does not mean that axial thermal stratification cannot be set in the scenario, particularly in the steam discharging bay. However, meshing axially the water region would entail an even stronger user effect. Definition of flowpaths and resistance flow coefficients to attempt to capture the highly complex fluid motion that might be set up (i.e., convection cells and buoyancy driven flows in the discharge bay, and distribution of the ascending hot water to the upper layer of adjacent locations), would pose a heavy modeling burden on the user. However, some parametric cases have been conducted to explore the potential impact of a "perfect axial stratification" (i.e., no involvement of the water layer under the SRV injection level).

4.1. Results

Given the nature of the present study, the major focus has been placed on containment variables, although some other complementary ones have been included to better illustrate the effects on the overall SBO analysis.

4.1.1. Pool thermal status

The variable that is more directly affected by wet well modeling is the suppression pool temperature. As noted in Fig. 5, the five cases explored show rather different evolutions. To begin with, when WW is modeled as a single node temperature (Fig. 5a) a progressive temperature increase (1 node legend) is estimated with the highest values around 60 K below the saturation temperature; in other words, pool water behaves as an efficient steam (and fission products) trap all over the sequence (i.e., until RPV failure).

As a matter of fact, the temperature slope changes describe phases of the accident. The first 1.7 h from scram, the IC works as designed and suppression pool remains at the initial conditions. After 1.7 h an SRV opens and a fraction of the steam being produced in the reactor as a consequence of decay heat, reaches the water bulk, condenses and the released latent heat is absorbed by water. This remains so for hours. However, at 4 h the temperature increase slows down because the amount of steam entering the pool decreases (a fraction of H_2O_v turns into H_2 within the reactor due mainly to Zr-H_2O_v oxidation). At about 6.2 h H_2 fraction in the gas coming from the RPV practically vanishes and pool temperature experiences a moderate jump, again due to H_2O_v condensation. From that time on, pool heat up slows down progressively as the water inventory in the reactor and, consequently, the amount of steam generated, decreases to nearly zero at the time of vessel failure (∼15.8 h).

When WW is broken down in 8 identical regions linked to each other by 1 flow path (Fig. 5a), the water in the node where the open SRV discharges (hereafter named WW1), heats up much faster than the others. In less than 3 h, it reaches the saturation level (dashed black line) for nearly a couple of hours (note that until reaching saturation other nodes hardly change their temperature). During that period, temperature at the other nodes group in couples and they grow according to their proximity to WW1 (i.e., WW2 and WW8 temperatures are similar and higher than WW3 and WW7). Then, when H_2 enters the containment it accumulates in the receiving WW1 space, slightly increasing its pressure until it gets transferred to its two neighbors (WW2 and WW8) and, occasionally, opens the WW1 vacuum breakers. Then, liquid mass exchange between nodes is noticeably enhanced, because of the combined gas/water flow which mixes the water pool as calculated (default momentum exchange terms are used). Thus, water from adjacent compartments (much colder than WW1's) gets into the WW1 and cools it down sharply, until temperature becomes uniform in the whole suppression pool. Such uniform temperature persists as long as H_2 keeps on flowing from RPV to containment. Once H_2 injection stops, the homogenous thermal state of the pool is lost and some differences raise again between different azimuthal locations. Nonetheless, the only relevant one is that of the WW1 with respect to others, since WW1 temperature increases again due to absorption of phase change enthalpy until reaching a pseudo steady state 10 K below saturation, while the others stay more than 50 K below at all times. The increase of WW1 water vanishes a little later than 11.5 h, as the steam flow rate into the pool is so small that water coming from adjacent nodes compensates any sort of

[1] L and V stand for a large volume of water and gas, respectively, whereas ℓ and v stand for small volumes of each phase (i.e., thin layers).

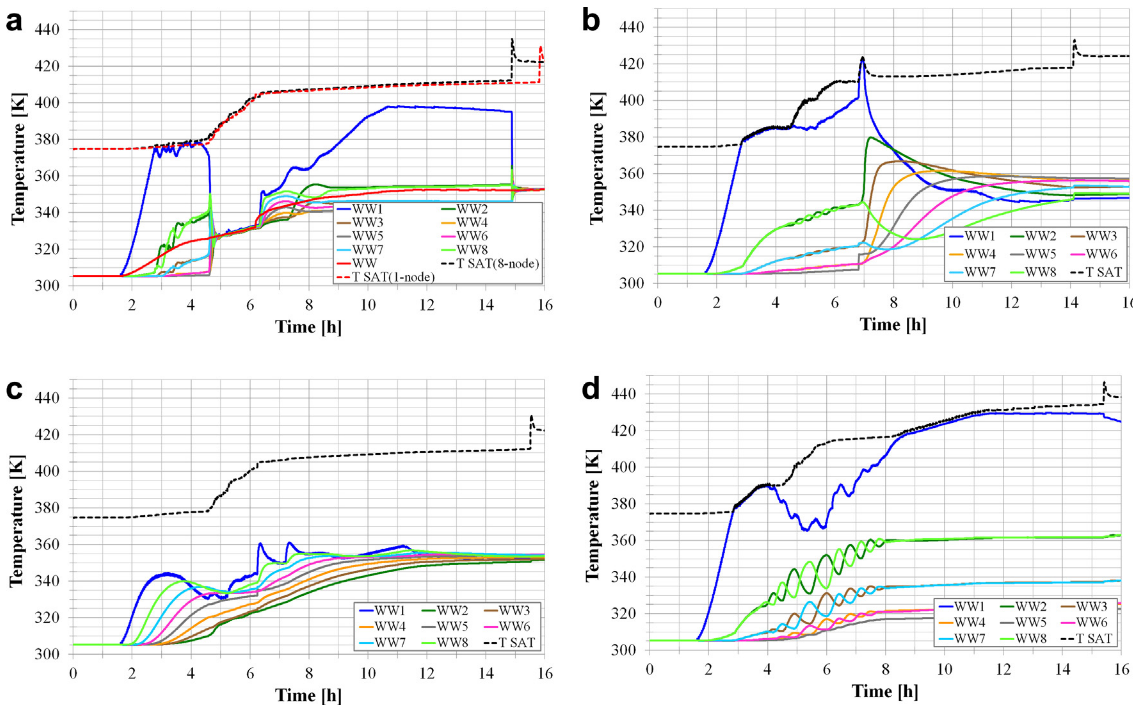

Fig. 5. Suppression pool temperature vs. time. (a) 1-node and 8-node 1 flow path cases. (b) 8-node Lv+V flow paths. (c) 8-node L+ℓV flow paths. (d) 8 × 2-node Lv+V flow paths.

heating up. At nearly 15 h, the RPV breaches (∼1 h before the single node case).

Fig. 5b (8 nodes with the Lv+V flow path arrangement) shows some apparent similarities with the case with a single flow path (for example, the rapid heat up of WW1 water up to saturation, or the grouping of other nodes' temperatures according to proximity to WW1), but they fade out as soon as H_2 injection starts. Despite similarity in the initial temperature evolution, there are also some significant differences, as the perfect match of saturation temperature, the slower heating up of nodes other than WW1, the high temperature that WW1 holds and even increases from 5 h to nearly 7 h, or the softer temperature drop when liquid flows become more meaningful ($t \sim 7$ h in the Lv+V case and $t \sim 4.5$ h in the single flow path case). These discrepancies are a consequence of the change that this configuration means in terms of in flow-path fluid exchanges: whereas the case shown in Fig. 5a entails a strong gas–water interaction, in this case (Fig. 5b) gas and water are decoupled, which is a scenario closer to reality than the "joint exchange" assumed in the single flow path case. As a result, in the Lv+V case the effect of H_2 on pool water temperature is notably smaller.

In Fig. 5c the results from the 8 nodes with the L+ℓV flow path arrangement has been displayed. This configuration enhances liquid mass exchanges from the early stages of the accident. Water displacement to other nodes makes WW1 temperature never reach saturation and other nodes start their temperature increase earlier than in the previous 8 node arrangements analyzed.

Finally, Fig. 5d shows the 8 × 2 nodes scenario (two flow paths, Lv+V). Until 4 h pool temperature evolves as in the 8 nodes Lv+V case. However, from the time that water in WW1 gets sub-cooled ($t \sim 4$ h), liquid exchanges between adjacent nodes become more intense than in the 8 node Lv+V case (the winding shape of WW2 and WW8 water temperature is a measure of the liquid exchange); this makes WW1 water to cool down due to water flows from other locations in the suppression pool. Once the H_2 injection stops, water heats up in a similar way as in the single flow path case, except that here WW1 temperature becomes saturated and that the gradient among other nodes is of nearly 40 K, compared to the hardly 15 K in the one single flow path case. As in that case, once steam condensation keeps on heating WW1 water, no mass exchange between nodes is enough to break down the thermal circumferential gradient set and pool temperature differences are higher than 100 K at the time RPV fails. This is exacerbated by the fact that, differently to other cases, separate HS definition in the upper and lower node of each azimuthal location, prevents from any gas–water heat transfer through HS. The straight consequence is that hot gas moving to the adjacent nodes takes a higher thermal energy load than in other configurations. In short, thermal-hydraulic differences between 8 nodes Lv+V and 8 × 2 nodes are not just affected by the noding scheme but also by the way HS have been modeled in those schemes. An example of such differences is the tendency of water temperature equalization in the long run observed in Fig. 5b and inexistent in Fig. 5d.

Experimental measurements taken in suppression pools of actual NPPs (Su, 1981) seemed to generally indicate no major circumferential thermal gradients in water volumes, except for the only Mark I containment tested (Monticello), in which noticeable temperature differences were found along the azimuth (>20 K). These findings might suggest the consistency of the 8-node L+ℓV flow paths configuration above. However, those observations cannot be directly applied to the scenario under investigation for several reasons: first, they correspond to transients, not to severe accident conditions; second, some key information is missing in many scenarios, like steam mass flux being discharged into the pool and duration of steam discharge; and, third, most containment types were not Mark I type. Therefore, from those measurements, no qualification of the different approaches analyzed can be made.

4.1.2. Containment pressure

The variable of highest interest in containment is pressure. Fig. 6 includes pressure evolution of the 5 cases explored in this study. As noted, despite the different behavior of water pool temperature

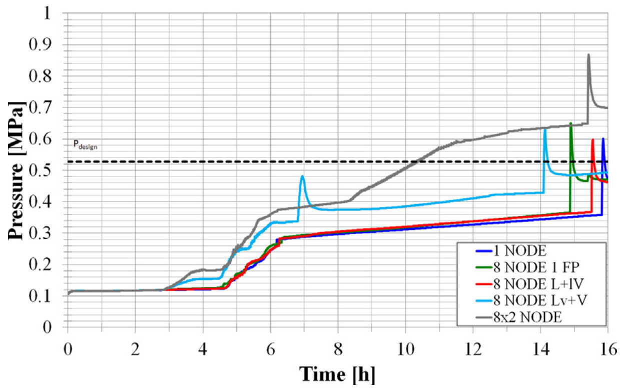

Fig. 6. Pressure evolution.

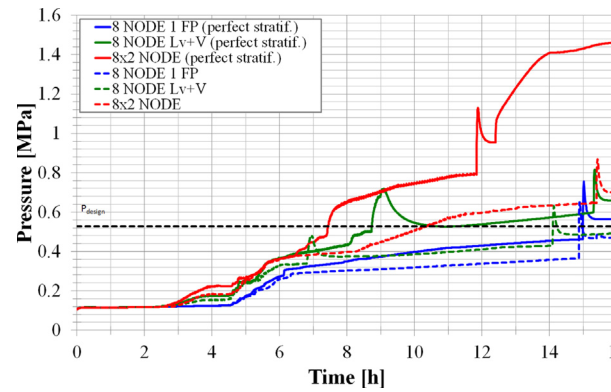

Fig. 8. Pressure evolution of "perfect axial stratification" cases.

discussed above, pressure develops in a practically identical way in the 1-node, 8-node 1 flow path, and 8-node 2 L+ℓV flow path cases. Pressure hardly rises until H_2 arrives the containment (at around 4.7 h); H_2 causes a 0.18 MPa increase in around 1.5 h and, then, a gentle increase occurs until RPV breaches. It is worth noting, though, that RPV fails at different times (within 1 h span, approximately) in each of those cases, but the resulting pressure spike is about 0.2 MPa (except in the 8-node single flow path case, that is around 0.3 MPa).

The 8-node Lv+V case behaved similarly, except that a first pressure step (0.04 MPa) happened before H_2 arrival; it was due to steam injection during the period in which water in the receiver WW node (WW1) was saturated. Then, H_2 is responsible for a significant pressure increase until 6 h. Later on, at a little earlier than 7 h (6.8 h), a pressure spike (pool gets back to saturation for a short time window) results from an additional gas injection from the RPV (H_2 and steam). From 7.3 h containment temperature increase drives a smooth pressure increase. The net pressure difference between this case and all of those with a common behavior is less than 0.1 MPa at the RPV failure time.

The 16 node case looks the most challenging as pressure escalates over 0.6 MPa at the RPV breach (15.4 h). The initial behavior of pressure is quite similar to the one of the 8-node 2 Lv+V flow paths case up to 6 h. Then pressure rise is driven by temperature increase in the containment except in between 8.3 h and 11.5 h. In this time period pool saturation makes steam from the RPV contribute to pressure raise at a higher rate than temperature does.

In order to complement what said above on pressure evolution, Fig. 7 shows DW temperature evolution. All the cases develop thermally in a similar way and end up at similar temperatures at any time before RPV breach. Therefore, as indicated above, pressure discrepancies come from differences concerning in-containment gas inventory. Generically, temperature unfolding may be described as follows: after a fast initial heat-up phase, DW temperature rises smoothly mainly due to natural convection from the RPV walls; the temperature slope changes when core is in an advanced degradation state and the RPV walls get hotter. As expected, RPV failure results in a DW temperature peak.

Finally, as said above, a set of parametric cases were run to assess the effect of preventing the water layer beneath the quenchers from any kind of exchange with the rest of water (i.e., a "perfect axial stratification"). The three cases correspond to those of 8 nodes and a single flow path, 8 nodes and two flow paths (Lv+V) and 8 × 2 nodes. Even though there are some slight differences in the thermal evolution of suppression pool, like faster temperature increases up to saturation in the discharge node, the major features of the water temperature history follow the same pattern as shown above, particularly those observations concerning circumferential stratification. Fig. 8 shows that in case of reaching a "perfect" axial thermal stratification, pressure levels would be substantially higher, particularly in those cases with two flow paths (less exchange between phases). In fact, maximum pressures before RPV breach might be more than 0.2 MPa higher than in the reference cases.

4.1.3. Overall discussion

Table 3 gives the in-RPV key event timing of the scenarios. As noted there, although there are some discrepancies, none of them make the scenarios explored become too different from the fuel degradation perspective as to hinder the comparisons set in terms of pool temperature and containment pressure and temperature.

As H_2 arrival at containment is a significant ingredient for pool behavior and containment pressure, Fig. 9 shows the H_2 injection history in the WW for the cases explored.

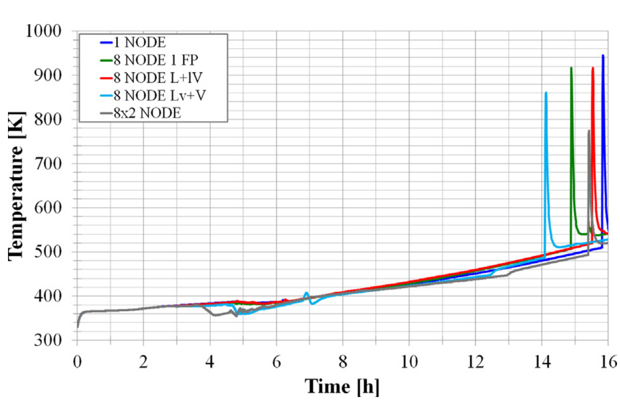

Fig. 7. DW temperature evolution.

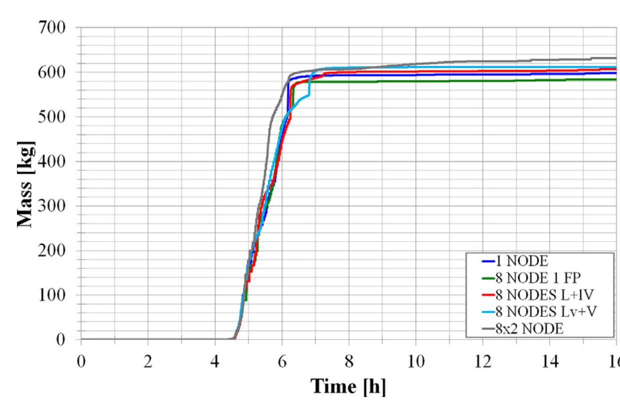

Fig. 9. H2 injection in the WW.

Table 3
Key events timing (h).

Key event	1 node	8 nodes 1 flow path	8 nodes Lv+V flow paths	8 nodes L+ℓV flow paths	8 × 2 nodes Lv+V flow paths
Core uncovery	3.1–4.8	3.1–4.7	3.0–4.8	3.1–4.8	3.1–4.9
Dry RPV	10.7	9.8	11.1	10.39	11.0
Fuel slump to lower plenum	6.2–17.3	6.2–15.6	5.2–16. 9	5.5–15.7	5.4–16.3
Vessel breach	15.8	14.9	15.5	14.1	15.4

In summary, when different WW nodalizations are used in a MELCOR 2.1 simulation of an SBO sequence in a BWR3 Mark I reactor, some significant magnitudes of the accident progression show a moderate scatter. This is the case, for instance, of in-core accident evolution, which timing remains similar, with onset of core uncovery at around 3 h and final vessel breach occurring between 14 h and 16 h. The same might be said concerning in-vessel H_2 generation, which has been estimated to be in the range of 600–700 kg in all the cases at the time of RPV failure. Differences become much more noticeable in the SP thermal state: some nodalization schemes indicate a large subcooling all over the sequence (i.e., 1-node approach), whereas in others substantial azimuthal thermal stratification is foreseen (some locations near or at saturation for long periods of time and others hardly ten degrees over the initial temperature). Fortunately, these large discrepancies fade away to a good extent when key containment variables, like pressure, are considered; those nodalizations using a specific Lv+V arrangement for the node-to-node exchanges show higher pressure values, and only when two vertical nodes in each circumferential sector are included (8 × 2 node configuration), discrepancies become outstanding.

It should be highlighted that all what said in the previous paragraph is applicable just to BWR3 Mark I designs whenever the severe accident results in a single injection location in the WW water. Whenever multiple injection locations become operative due to activation of systems like RHR, HPCI and/or RCIC (BWR4), the likelihood for stratification should be smaller and the feedback between PCV and RPV might be strongly affected, so that accident progression might change significantly. Therefore, extrapolation of the above results and discussions, other than the interest of conducting sensitivity analyses on the WW nodalizations effect, should not be made.

5. Final remarks

The deep effect that a code user may have when simulating a severe accident scenario is well known. One of the most challenging aspects of NPP modeling is, beyond any doubt, nodalization. It is worth noting that even if focused on a specific WW phenomenon at a given location (i.e., stratification in the suppression pool), the detailed nodalization of WW has been consistently balanced by a detailed plant meshing.

The above section has illustrated how key containment variables, like pressure, might behave depending on suppression pool thermal state, which is in turn a strong function of wet well nodalization. Given the relevance of the Fukushima accident, the scenario addressed has been an SBO in a BWR3 Mark I. Nonetheless, the presence of multi-hole spargers in advanced NPP is drawing attention to phenomena closely related to the present study (Park et al., 2007). It should be underlined that despite the present study is focused on thermal-hydraulic variables; other magnitudes such as SP decontamination efficiency might also be heavily impacted.

The analysis conducted allows discussing advantages and disadvantages of the essentially two approaches tested (i.e., single vs. multiple nodes):

- A single node approach is the simplest way to proceed, so that code users are not challenged with options and/or assumptions to be made. On the other side, it implicitly involves an instantaneous uniform distribution of the enthalpy injected in the water bulk of the pool; as a consequence, water temperature is the lowest possible at the injection point or, in other words, a non-conservative approximation to the pool thermal state.
- A multiple mesh approach provides the model with some flexibility that there might result in capturing scenario features impossible to catch with a single node. In exchange, the user faces the tough task of deciding on arbitrary options, as the number of nodes, their azimuthal and vertical distribution, or the characteristics of flow paths through which adjacent nodes exchange mass and energy. No less important, the user has to set some values in the input deck for physical model parameters that very often are uncertain.

Adopting any of these approaches should be done carefully and based on a deep understanding of the phenomena expected and the ways offered by the code to deal with them. The analyst should be aware of drawbacks of the approach taken and cautiously examine code estimates to make it sure that no unphysical behavior has been caused by the different user options set or parameters defined.

A number of insights into WW nodalization of BWR3 Mark I containments undergoing an SBO severe accident has been gained and is summarized as follows:

- A single node assumption for the whole WW would prevent some key phenomena from being predicted (as thermal stratifications) and, as a consequence, result in a wrong estimate of PCV pressurization.
- Given the drift model used for the momentum exchange between phases along flow paths in MELCOR 2.1, a strong coupling of both phases seems not to be desirable, so that either a separate transport of the main body of both phases (8 node Lv+V or 8 × 2 nodes Lv+V) and/or a shorter momentum exchange length are recommended.
- The axial potential stratification should be accounted for as a potential phenomenon to be captured by any nodalization to be intended. Otherwise, if it eventually happened, a non-conservative pool temperature would be estimated.
- Given the sensitivity of results to the nodalization schemes, a sort of uncertainty and/or sensitivity analysis focused on key magnitudes describing containment evolution, like pressure, should be conducted with those more uncertain and highly influencing parameters.

Finally, consistently with some experimental programs aimed at studying vertical stratification in SP (i.e., POOLEX – Laine et al., 2011), an experimental project to explore potential circumferential stratification in SP during SBO accidents might be timely as well, particularly for the scenario investigated in this work. Based on the measurements there made, approaches like those tested in this study and/or others might be qualified, refined or neglected.

Acronyms

AC	alternating current
ADS	automatic depressurization system
BDBA	beyond design-basis accident
BSAF	benchmark study of the accident at the Fukushima Daiichi Nuclear Power Station
BWR	boiling water reactor
CDF	core damage frequency
DC	direct current
DW	dry well
FCV	filtered containment venting
FP	flow path
HPCI	high pressure coolant injection
HS	heat structure
IC	isolation condenser
MSIV	main steam isolation valve
NPP	nuclear power plant
PAR	passive autocatalytic recombiner
PCV	primary containment vessel
RB	reactor building
RCIC	reactor core isolation cooling
RCS	reactor cooling system
RHR	reactor heat removal
RPV	reactor pressure vessel
SBO	station blackout
SFP	spent fuel pool
SP	suppression pool
SRS	safety relief system
SRV	safety-relief valve
STSBO	short term SBO
SV	safety valve
VB	vacuum breaker
WW	wet well

Acknowledgments

The authors thank the Spanish Nuclear Safety Council (CSN) for their financial support under the research and development agreement (CSN-ACAS) on severe accidents. Particularly to F. Robledo whose remarks highlighted some of the issues discussed above.

References

Birchley, J., Fernández-Moguel, L., 2012. Simulation of air oxidation during a reactor accident sequence: Part 1 – Phenomenology and model development. Ann. Nucl. Energy 40, 163–170.

Bixler, N., Gauntt, R., Jones, J., 2013. State-of-the-Art Reactor Consequence Analyses Project. Volume 1: Peach Bottom Integrated Analysis. NUREG/CR-7110.

Carbajo, J.J., 1994. MELCOR sensitivity studies for a low-pressure, short term station blackout at the Peach Bottom plant. Nucl. Eng. Des. 152, 287–317.

Clément, B., Haste, T., 2004. ISP-46 – PHEBUS FPT-1 integral experiment on reactor severe accidents. NEA/CSNI/R(2004)18.

Cook, D.H., 1984. Calculation of thermal mixing for the BWR Mark I containment pressure suppression pool. CONF-8410142-10.

EC, 2012. On the comprehensive risk and safety assessments ("stress tests") of nuclear power plants in the European Union and related activities. Communication from the Commission to the Council and the European Parliament, COM(2012) 571, http://ec.europa.eu/energy/nuclear/safety/stress_tests_en.htm.

Gauntt, R.O., Cole, R.K., Erickson, C.M., Gido, R., Gasser, R.D., Rodriguez, S.B., Young, M.F., 2011. MELCOR Computer. Code Manual. Sandia National Laboratories, NUREG/CR-6119, Vol. 1, Rev 3179.

Gauntt, R., Kalinich, D., Cardoni, J., Phillips, J., Goldmann, A., Pickering, A., 2012. Fukushima Daiici Accident Study (Status as of April 2012). SAND2012-6173.

Hanson, D.J., Blackman, H.S., Nelson, W.R., Wright, R.E., Leonard, M.T., Disalvo, R., 1988. Analysis of containment venting at the Peach Bottom atomic power station. Nucl. Eng. Des. 108, 71–81.

Herranz, L.E., García, M., López, C., Fontanet, J., 2012a. Pool scrubbing in Fukushima-like scenarios: modeling status and major challenges. In: The 9th International Topical Meeting on Nuclear Thermal-Hydraulics, Operation and Safety (NUTHOS-9), Kaohsiung, Taiwan, September 9–13.

Herranz, L.E., López, C., García, M., 2012b. From a LOOP to a Fukushima-like SBO: assessment of the effect of BWR3-MarkI Safety Systems. In: ANS meeting 2012, Topical Meeting "Fukushima", San Diego (EEUU), November 11–15.

Herranz, L.E., Albiol, T., Riera, E., Guieu, S., Lind, T., Morandi, S., Rantanen, P., Losch, N., Finqueneisel, G., 2014. Technical bases for experimentation on source term mitigation: the EU-PASSAM Project. In: 10th International Topical Meeting on Nuclear Thermal-Hydraulics, Operation and Safety (NUTHOS-10), Okinawa, Japan, December 14–18.

Jones, A.V., Dickinson, S., Pascale, C., Hanniet, N., Herranz, L.E., de Rosa, F., Henneges, G., Langhans, J., Housiadas, C., Wichers, V., Birchley, J., Paci, S., Martin-Fuertes, F., 2003. Validation of severe accident codes against PHEBUS FP for plant applications: status of the PHEBEN2 project. Nucl. Eng. Des. 221, 225–240.

Laine, J., Puustinen, M., Räsänen, A., Tanskanen, V., 2011. PPOOLEX experiments on stratification and mixing in the wet well pool. NKS-240, ISBN 978-87-7893-312-6.

Lee, M., Lee, G.D., 1992. Quantification of severe accident source terms of BWR4 reactor with Mark I containment using source term code package. Nucl. Eng. Des. 138, 313–337.

Leonard, M.T., Gauntt, R.O., Powers, D.A., 2007. Accident source terms for boiling water reactors with high burnup cores calculated using MELCOR 1.8.5. SAND2007-7697.

Mizokami, S., Yamada, D., Honda, T., Yamauchi, D., Yamanaka, Y., 2014. Unsolved issues relating thermal-hydraulics in the suppression chamber during Fukushima Daiichi accident. In: The 9th International Topical Meeting on Nuclear Thermal-Hydraulics, Operation and Safety (NUTHOS-9), Kaohsiung, Taiwan, September 9–13.

NAIIC (The National Diet of Japan), 2012. The Fukushima nuclear accident independent investigation commission.

NEA, 2012. http://www.oecd-nea.org/jointproj/bsaf.html.

NEA, 2013. SFP project concluding seminar 2013. NEA/CSNI/R(2013).

Ott, L.J., 1989. Advanced severe accident response models for BWR application. Nucl. Eng. Des. 115, 289–303.

Park, C.K., Song, C.H., Jun, H.G., 2007. Experimental investigation of the steam condensation phenomena due to a multi-hope sparger. Nucl. Sci. Technol. 44, 548–557.

Park, S.-Y., Ahn, K.-I., 2012. Comparative analysis of station blackout accident progression in typical PWR, BWR and PHWR. Nucl. Eng. Technol. 44 (3), 311–322.

Patterson, B.J., 1979. Mark I Containment Program. Monticello T-Quencher thermal mixing test. Final Report, NEDO-24542.

Schwarz, S., Fischer, K., Bentaib, A., Burkhardt, J., Lee, J.J., Duspiva, J., Visser, D., Kyttälä, J., Royl, P., Kim, J., Kostka, P., Liang, R., 2011. Benchmark on hydrogen distribution in a containment based on the OECD-NEA THAI HM-2 experiment. Nucl. Technol. 175, 594–603.

Su, T., 1981. Suppression pool temperature limits for BWR containments. NUREG-0783.

U.S. NRC, 1975. Reactor Safety Study: An Assessment of Accident Risks in U.S. Commercial Nuclear Power Plants. NUREG-75/014WASH-1400.

U.S. NRC, 1990. Severe accident risks: an assessment for five US nuclear power plants. NUREG-1150.

U.S. NRC, 2005. Reevaluation of Station Blackout risk at nuclear power plants. NUREG/CR-6890.

Van Dorsselaere, J.P., Chatelard, P., Chevalier-Jabet, K., Nowack, H., Herranz, L.E., Pascal, G., Sanchez-Espinoza, V.H., 2015. ASTEC code development, validation and applications for severe accident management within the CESAM European project. In: International Congress on Advanced nuclear Power Plants (ICAPP 2015), May 3–6, Nice, France.

Wallis, G.B., 1969. One-dimensional two-phase flow. In: The Drift Flux Model. McGraw Hill Inc (Chapter 4).

Weber, G., Herranz, L.E., Bendiab, M., Fontanet, J., Funke, F., Gonfiotti, B., Ivanov, I., Krajewski, S., Manfredini, A., Paci, S., Pelzer, M., Sevón, T., 2013. Thermal-hydraulic-iodine chemistry coupling: insights gained from the SARNET benchmark on the THAI experiments IOD-11 and IOD-12. Nucl. Eng. Des. 265, 95–107.

Zhao, H., Zou, L., Zhang, H., 2014. Simulation of thermal stratification in BWR suppression pools with one dimensional modeling method. Ann. Nucl. Energy 63, 533–540.